Available online at www.sciencedirect.com
SCIENCE DIRECT®
Journal of Catalysis 222 (2004) 368–376
JOURNAL OF CATALYSIS
www.elsevier.com/locate/jcat

Ag cluster as active species for SCR of NO by propane in the presence of hydrogen over Ag-MFI

Junji Shibata,[a] Yuu Takada,[a] Akira Shichi,[a] Shigeo Satokawa,[b] Atsushi Satsuma,[a,*] and Tadashi Hattori [a]

[a] *Department of Applied Chemistry, Graduate School of Engineering, Nagoya University, Chikusa-ku, Nagoya 464-8603, Japan*
[b] *Technical Research Institute, Tokyo Gas Co., Ltd., 16-25 Shibaura-1, Minato-ku, Tokyo 105-0023, Japan*

Received 9 June 2003; revised 7 November 2003; accepted 18 November 2003

Abstract

The effect of the addition of H_2 on SCR of NO by C_3H_8 over Ag-MFI was studied. SCR activity over Ag-MFI was significantly enhanced by the addition of H_2 below 673 K. Upon the removal of H_2 from reaction gases, NO reduction activity decreased to the same conversion before the addition of H_2, indicating that the promotion effect of H_2 on NO reduction activity was reversible. UV-vis spectroscopy was used to identify the active structure of Ag species during the C_3H_8-SCR. Ag^+ ion was mainly in existence during the C_3H_8-SCR in the absence of H_2, while $Ag_n^{\delta+}$ clusters ($2 \leqslant n \leqslant 4$), together with Ag^+ ion, were formed in the presence of H_2. NO reduction rate and band intensity due to the $Ag_n^{\delta+}$ cluster increased with an increase in H_2 concentration. On the other hand, formation of a metallic Ag_m cluster ($3 \leqslant m \leqslant 5$) and Ag metal increased the contribution of nonselective hydrocarbon combustion to the overall reaction. From the above results, it is indicated that a moderately agglomerated $Ag_n^{\delta+}$ cluster is a highly active species for the SCR by C_3H_8 in the presence of H_2, and that the role of H_2 is reduction of Ag^+ ion to $Ag_n^{\delta+}$ clusters. Ag species is markedly influenced by concentrations of gaseous components not only H_2 but also NO and C_3H_8. In addition, the type of Ag species was reversibly changed among Ag^+ ion, $Ag_n^{\delta+}$ clusters, and metallic Ag_m clusters together with Ag metal, depending on the reaction atmosphere, which suggests that gaseous components control the balance among Ag species on the catalyst.

Keywords: HC-SCR; Ag-MFI; H_2; Active species; UV-vis; Ag cluster

1. Introduction

A selective catalytic reduction of NO by hydrocarbons (HC-SCR) in the presence of excess oxygen is a potential method for removing NO_x from lean-burn and diesel exhausts. Since the pioneering work of Iwamoto et al. [1] and Held et al. [2], extensive research has been done on the development of de-NO_x catalysts and many types of zeolite-based catalyst have been reported [3–5]. Ag has attracted much attention since Miyadera reported a high activity of the SCR by ethanol over Ag/Al_2O_3 [6]. Ag-containing zeolites are known as active catalysts above 673 K for SCR of NO by light hydrocarbons including CH_4 [4,5,7–11]. In addition, for SCR of NO by $(CH_3)_2O$, Ag-containing zeolites were active in the range of 498 to 723 K, but the activity of the catalysts was low [9,10]. Although the addition of other elements such as Ce [7,8] and Pd [10] into the catalysts was attempted in order to enhance SCR activity, a drastic enhancement of SCR activity was not achieved.

We recently reported a drastic enhancement of NO reduction activity at lower temperatures by the addition of a small amount of H_2 for SCR by light hydrocarbons over Ag/Al_2O_3 [12–14]. Moreover, we investigated the promotion effect of H_2 on surface steps in SCR by C_3H_8 over Ag/Al_2O_3 with in situ IR spectroscopy and clarified that the promotion effect was mainly attributed to the remarkable promotion of partial oxidation of C_3H_8 to surface acetate, which is one of the important adspecies for producing N_2 for HC-SCR over the catalyst [14]. In order to fully elucidate a mechanistic cause of this attractive promotion effect, investigation of Ag species as an active species is also indispensable. H_2 has an ability to reduce Ag^+ ion to Ag clusters and Ag metals at relatively low tempera-

* Corresponding author.
E-mail address: satsuma@apchem.nagoya-u.ac.jp (A. Satsuma).

0021-9517/$ – see front matter
doi:10.1016/j.jcat.2003.11.007

tures [15–17]. Very easy formation of Ag clusters, having absorption bands at 304 and 368 nm, was observed over Ag/Al_2O_3 under a flow of 0.5% H_2 in the presence of 10% O_2 with in situ UV-vis spectroscopy [18]. Moreover, it is reported that Ag^+ ion are reduced to metallic Ag under the C_3H_6-SCR atmosphere [19,20]. Considering these reports, it is expected that Ag species is reduced by H_2 under a HC-SCR atmosphere over Ag catalysts and reduced Ag species is the highly active species for NO reduction. However, the details of active reduced Ag species are not determined and the influence of the gas composition on Ag species under steady-state HC-SCR conditions is not clearly reported.

Because of optical absorption due to Al_2O_3 itself below 300 nm [20], it is difficult to observe Ag species that have UV absorption bands below 300 nm. Therefore, Al_2O_3 support is not suitable for determination of active Ag species for SCR of NO with UV-vis spectroscopy. On the other hand, for Ag-containing zeolites [8,21–24], the bands due to various structures of Ag species (Ag^+ ion, Ag clusters, and Ag metal) including those below 300 nm are distinguishable in the UV-vis spectra. Reversible transformation of Ag species was reported on Ag ion-exchanged zeolites under unsteady-state conditions [15–17,25]. Thus, zeolite supports are suitable for the determination of active reduced Ag species for the HC-SCR and investigation of the influence of the gas composition on Ag species under steady-state conditions.

In this study, we first confirm enhancement of the C_3H_8-SCR activity by the coexistence of H_2 over Ag-containing MFI-type zeolite catalysts. Moreover, Ag species in the C_3H_8-SCR on Ag-MFI is investigated using UV-vis spectroscopy and details of the active reduced Ag species and a balance of various Ag species under C_3H_8-SCR are discussed.

2. Experimental

H-MFI ($Si/Al = 22$), supplied from Tosoh Co., was used as the parent zeolite. Ag-MFI was prepared from H-MFI by ion exchange with an aqueous $AgNO_3$ solution at room temperature [7,8,11]. After filtration, the sample was washed with distilled water and dried at 393 K, followed by calcination at 773 K for 6 h in flowing dried air. The final samples were analyzed by inductively coupled plasma emission spectroscopy (ICP, Jarrel-Ash Model 975) to determine their elemental composition. Unless otherwise noted, Ag-MFI with a Ag exchange level of 58% (Ag-MFI-58) was used for reaction tests and characterizations.

The catalytic test was performed with a fixed-bed flow reactor by passing a mixture of 0.1% (1000 ppm) NO, 0.1% (1000 ppm) C_3H_8, 10% O_2, and 0.5% H_2 in He at a rate of 100 $cm^3\,min^{-1}$ over 0.2 g catalyst (GHSV = 19,000 h^{-1}). Prior to the experiment the catalyst was heated in 10% O_2/He at 773 K for 1 h. After reaching steady state, the effluent gas was analyzed by gas chromatography and a NO_x analyzer (Best BCL-100uH). The reaction results were described in terms of NO conversion to N_2, hydrocarbon conversion to CO_x, and H_2 conversion and selectivity defined below. N_2O was barely detected (below 5%). In addition, CH_4, C_2H_6, and C_2H_4 were not detected at reaction temperatures below 723 K, and hence hydrogenolysis and cracking of C_3H_8 should be neglected. The selectivity was defined as the ratio of oxygen atoms supplied from NO to all oxygen atoms reacting with hydrocarbons to CO and CO_2 [26]. The selectivity is represented as $2 \times N_2/[7/3 \times CO + 10/3 \times CO_2] \times 100$ (%). The selectivity is equal to 100% in the case of complete selective oxidation of C_3H_8 by NO, and it decreases as the contribution of C_3H_8 combustion by O_2 increases.

Diffuse reflectance UV-vis spectra of catalysts were measured with a JASCO V-570. The sample was exposed to various gas mixtures at 573 K and quenched at room temperature. Then, UV-vis spectra of the quenched sample were measured after being moved into an optical quartz cell without exposure to the air. Powder X-ray diffraction (XRD) patterns of powdered catalysts were obtained with Rigaku RINT 1200 using Cu-K_α radiation filtered by Ni.

3. Results

3.1. C_3H_8-SCR activity in the presence of H_2 and Ag species

Fig. 1 shows the conversions of NO and C_3H_8 for C_3H_8-SCR in the absence and presence of 0.5% H_2 over Ag-MFI-58 as a function of temperature. Clearly, both conversions of NO and C_3H_8 were increased significantly by the addition of H_2 below 673 K. A maximum NO conversion of 48% was obtained at 573 K where H_2 conversion reached nearly 100%, and an increase in C_3H_8 conversion by the addition of H_2 was the highest at 573 K (from 8 to 50%). In a $NO + H_2 + O_2$ reaction, reduction of NO was not observed in the range of 448 to 773 K (result not shown).

Fig. 2 shows C_3H_8 conversions for C_3H_8 combustion ($C_3H_8 + O_2$) in the absence and presence of 0.5% H_2 over Ag-MFI-58 in addition to those for the C_3H_8-SCR shown in Fig. 1B. Clearly, C_3H_8 conversion for the C_3H_8 combustion was also increased by the addition of H_2 below 723 K. It should be noted that C_3H_8 conversions for the C_3H_8 combustion are lower than those for the C_3H_8-SCR regardless of the presence of H_2.

Fig. 3 shows the time dependence of NO conversion for the C_3H_8-SCR in the absence and presence of H_2 at 573 K over Ag-MFI-58. The catalytic activity was very low (5%) for 120 min in a flow of $NO + C_3H_8 + O_2$. Upon the addition of H_2 in reaction gases, NO conversion immediately increased and finally reached to 48%, which agreed with the steady-state NO conversion at 573 K in the presence of H_2 (Fig. 1). Upon the removal of H_2 from reaction gases, NO conversion decreased immediately and returned to the same conversion before the addition of H_2. Further removal and

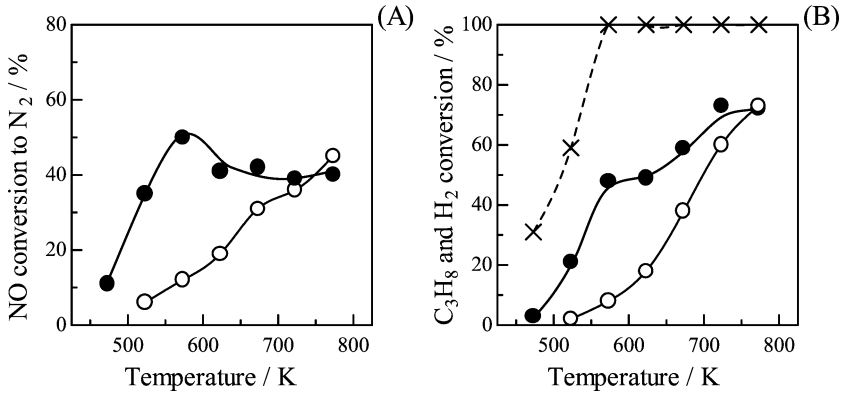

Fig. 1. (A) NO conversion to N_2 and (B) C_3H_8 conversion to CO_x for C_3H_8-SCR in the (●) presence and (○) absence of 0.5% H_2 over Ag-MFI-58. Cross symbol (×) denotes H_2 conversion.

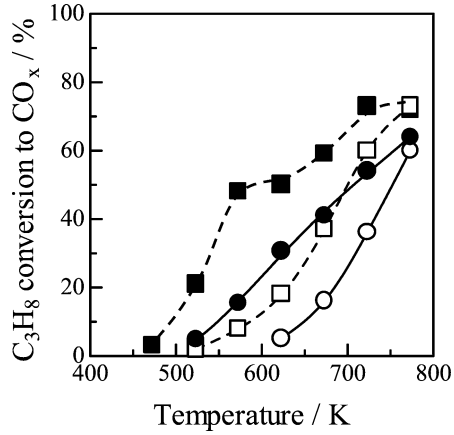

Fig. 2. C_3H_8 conversion to CO_x for (■, □) C_3H_8-SCR and (●, ○) C_3H_8 combustion in the (■, ●) presence and (□, ○) absence of H_2 over Ag-MFI-58.

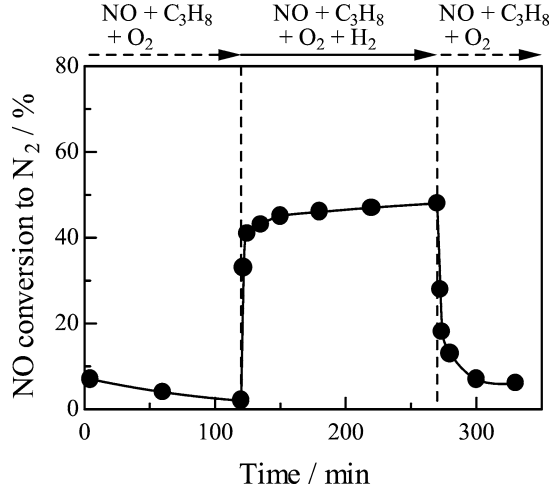

Fig. 3. Time dependence on NO conversion for C_3H_8-SCR in the absence and presence of 0.5% H_2 over Ag-MFI-58.

addition of H_2 also resulted in reversible change in the NO conversion.

Fig. 4 shows UV-vis spectra of Ag-MFI-58 after pretreatment under various atmospheres at 573 K followed by

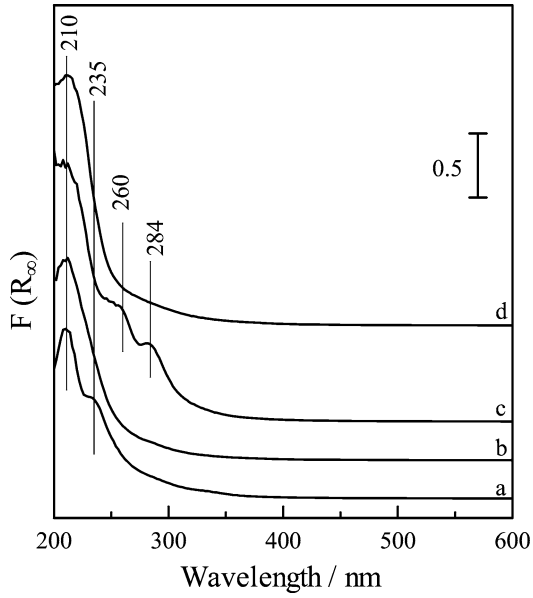

Fig. 4. UV-vis spectra of Ag-MFI-58 after a flow of (a) O_2 at 773 K for 1 h, (b) NO + O_2 + C_3H_8 at 573 K for 30 min, (c) NO + O_2 + C_3H_8 + H_2 at 573 K for 30 min and (d) NO + O_2 + C_3H_8 at 573 K for 30 min after (c). Conditions: NO = 0.1%, C_3H_8 = 0.1%, O_2 = 10% and H_2 = 0.5%.

quenching at room temperature. Bands at 210 and 235 nm were observed after pretreatment in a flow of 10% O_2 at 773 K (spectrum a). The observation of these bands was also reported for Ag/Al_2O_3 [19,20,27–29] and Ag ion-exchanged zeolite catalysts [8,21–23], and they were assigned to the $4d^{10}$ to $4d^9s^1$ transition of Ag^+ ion. Texter et al. reported that the UV absorption bands due to trigonally coordinated Ag^+ ion were observed as a triplet centered at 5.55 eV (223 nm) [23]. This means that the same Ag^+ ion gives plural bands. In our present study, the two absorption bands in the UV-vis spectrum may be ascribed to the same Ag^+ ion. After the SCR in the absence of H_2, no other absorption bands appeared, although the band at 235 nm disappeared (spectrum b). Texter et al. reported that UV absorption bands of Ag^+ ion were observed as a clear triplet (192, 210, and 225 nm) in H_2O while the band intensity at 225 nm among the triplet was remarkably lower in ethanol [30]. Consider-

ing their report, the disappearance of the band at 235 nm may be attributed to adsorption of gases (e.g., NO_x and H_2O) on Ag^+ ion. Thus, the UV-vis spectrum b indicates that Ag^+ ions are the predominant Ag species under C_3H_8-SCR in the absence of H_2. Then, by the addition of 0.5% H_2 for 30 min, new bands at 260 and 284 nm were observed (spectrum c). Henglein and co-workers assigned the absorption band around 280 nm to Ag_4^{2+} in the studies on the pulse radiolytic reduction of Ag ions in aqueous solutions [31–33]. In a study on γ-irradiated AgCs-rho zeolites, Michalik et al. assigned the absorption band at 270 and 282 nm to Ag_4^{2+} and Ag_4^{3+}, respectively [24]. Gachard et al. reported the formation of Ag_3^{2+} (265 nm) through γ-irradiation to AgNa-Y zeolites [34]. Sato et al. assigned the bands in the range of 238–272 and 275–326 nm to $Ag_n^{\delta+}$ and Ag_{n1} clusters, respectively [29]. The assignment of the latter band is similar to that observed for 5 wt% Ag/Al_2O_3 in our previous report [27]. However, since this band is very broad, it may include a band due to a $Ag_n^{\delta+}$ cluster around 285 nm. Therefore, we have assigned the new species observed at 260 and 285 nm to a $Ag_n^{\delta+}$ cluster ($2 \leqslant n \leqslant 4$). The sample was further treated under the C_3H_8-SCR in the absence of H_2 for 30 min. The bands of the $Ag_n^{\delta+}$ cluster disappeared after this treatment (spectrum d), and spectrum d coincided with spectrum b before the addition of H_2.

3.2. Influence of H_2 concentration

Fig. 5 shows the NO and C_3H_8 conversion and selectivity for the C_3H_8-SCR in the presence of H_2 as a function of H_2 concentration at 573 K. Conversions of both NO and C_3H_8 increased by the addition of 0.15% of H_2. NO conversion increased with an increase in H_2 concentration to 1%, and decreased gradually with a further increase in H_2 concentration. On the other hand, C_3H_8 conversion monotonously increased with an increase in H_2 concentration. As a result,

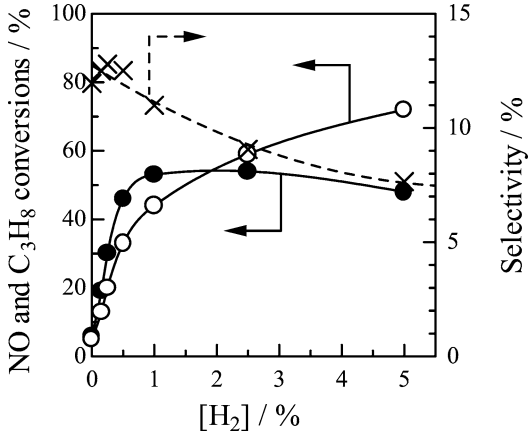

Fig. 5. Dependence of H_2 concentration on (●) NO conversion to N_2, (○) C_3H_8 conversion to CO_x, and (×) selectivity for C_3H_8-SCR in the presence of H_2 over Ag-MFI-58 at 573 K. Conditions: NO = 0.1%, C_3H_8 = 0.1%, and O_2 = 10%.

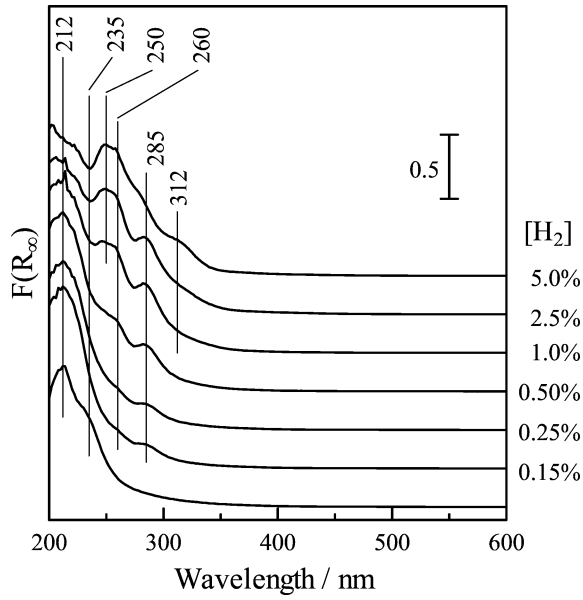

Fig. 6. UV-vis spectra of Ag-MFI-58 after a flow of NO + O_2 + C_3H_8 + H_2 at 573 K for 30 min. H_2 concentration was varied from 0 to 5%.

the selectivity decreased monotonously with the increase in H_2 concentration.

Fig. 6 shows UV-vis spectra of Ag-MFI-58 after treatment in an SCR atmosphere with various H_2 concentrations. The band due to the $Ag_n^{\delta+}$ cluster (260 and 285 nm) appeared after the C_3H_8-SCR in the presence of 0.15% of H_2. The band intensities of the $Ag_n^{\delta+}$ cluster increased with an increase in H_2 concentration below 1%. New bands at 250 and 312 nm appeared at H_2 concentrations above 1%. The absorption bands at 300 and 330 nm were assigned to Ag_3 and Ag_5 by Henglein et al., respectively [31,32]. Mitchell and Ozin observed an absorption band due to Ag_3 around 250 nm in a study on thermal and photochemical silver atom aggregation reactions in rare gas matrices [35]. Since these bands at 250 and 312 nm in Fig. 6 appeared under higher H_2 concentrations than those of $Ag_n^{\delta+}$ clusters, assignment of these bands to metallic Ag clusters such as Ag_3 is reasonable. Therefore, we tentatively assigned the bands at 250 and 312 nm to metallic Ag_m clusters ($3 \leqslant m \leqslant 5$), although the assignment of these bands to a cationic cluster which is larger or more neutral than a $Ag_n^{\delta+}$ cluster is not excluded.

3.3. Influence of pretreatment by H_2

After the treatment of Ag-MFI-58 in a flow of 100% H_2 at 773 K for 1 h, the SCR by C_3H_8 was carried out in the presence of H_2. Fig. 7 shows the time dependence of NO conversion, C_3H_8 conversion, and selectivity. Just after the treatment in H_2 (5 min in Fig. 7), NO conversion was nearly zero, while C_3H_8 conversion was sufficiently high (34%), indicating that only nonselective C_3H_8 oxidation proceeds on the catalyst after deep reduction. Then, NO conversion increased markedly with time on stream and approached the same level shown in Fig. 1. On the other hand, C_3H_8 con-

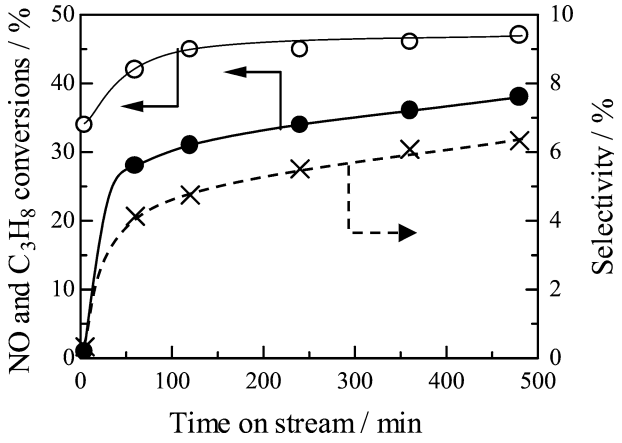

Fig. 7. Time dependence on (●) NO conversion to N_2, (○) C_3H_8 conversion to CO_x and for C_3H_8-SCR over Ag-MFI-58 in the presence of 0.5% H_2 after 100% H_2 treatment at 773 K for 1 h.

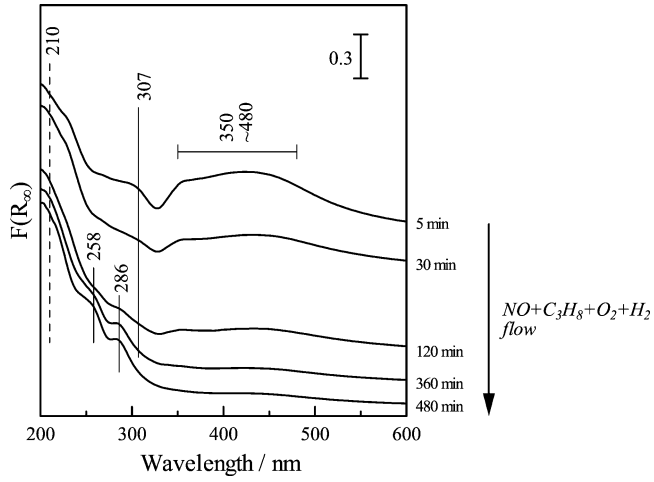

Fig. 8. Changes in the UV-vis spectra of Ag-MFI-58 as a function time after a flow of NO + O_2 + C_3H_8 + H_2 at 573 K. Before the measurement, the catalyst was treated with 100% H_2 at 773 K for 1 h. Conditions: NO = 0.1%, C_3H_8 = 0.1%, O_2 = 10%, and H_2 = 0.5%.

version was at first 34% and then increased gradually until 120 min.

It is well-known that Ag metal on the external surface of Na-Y is formed by H_2 at temperatures much lower than 773 K [15–17]. H_2 treatment at 773 K in our present study should be sufficient to form Ag metal particles on Ag zeolites. Actually, diffraction lines due to Ag metal particles at $2\theta = 38.1$, 44.3, and 64.5° were observed in an XRD pattern of Ag-MFI-58 after H_2 treatment at 773 K. The size of the Ag metal particle was estimated roughly as 40 nm from the Scherrer equation, which was much bigger than the pore size of MFI. Fig. 8 shows the time dependence of the UV-vis spectra of this reduced Ag-MFI-58 under a flow of NO + C_3H_8 + O_2 + H_2 at 573 K. After a flow of NO + C_3H_8 + O_2 + H_2 for 5 min, a band due to a metallic Ag_m cluster at 307 nm and a broad band from 340 to 480 nm were observed. The broad band from 340 to 480 nm was assigned to Ag metal (plasma resonance absorption

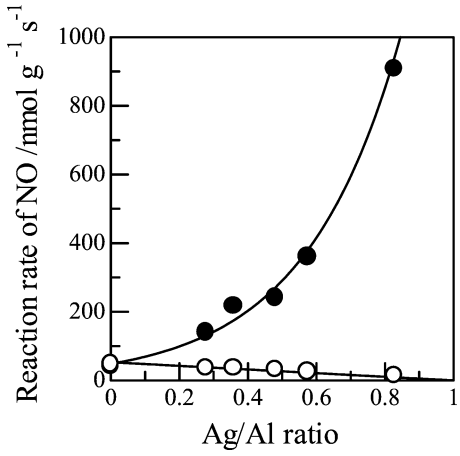

Fig. 9. NO reduction rate toward Ag/Al ratio for the C_3H_8-SCR over Ag-MFI in the (○) absence and (●) presence of 0.5% H_2 at 573 K.

band) [18–22,28], which supported the presence of Ag metal particles obtained by XRD patterns. With time on stream, the intensities of new bands due to the $Ag_n^{\delta+}$ cluster (258 and 286 nm) increased in contrast to gradual decreases in those of the bands due to metallic Ag_m clusters and Ag metal. A spectrum after 480 min was similar to spectrum b in Fig. 4 except that the absorption of Ag metal remained slightly. Migration of Ag metal particles into the zeolite occurs by O_2 treatment above 500 K [15,36] and evacuation at 303 K [17] for AgNa-Y. Considering these reports, our result indicates that the metallic the Ag_m cluster and Ag metal are oxidized to a $Ag_n^{\delta+}$ cluster during the SCR in the presence of H_2.

3.4. Influence of Ag/Al ratio on C_3H_8-SCR activity

The influence of the Ag/Al ratio on C_3H_8-SCR activity was examined. Fig. 9 shows the reaction rate of NO for C_3H_8-SCR in the absence and presence of H_2 at 573 K as a function of Ag/Al ratio. It should be noted that the reaction rate was measured in the conversion level of the reactants lower than 50% by varying catalyst weight. The reaction rate over H-MFI (Ag/Al = 0) did not change by the addition of H_2. The reaction rate decreased linearly with Ag/Al ratio in the absence of H_2. On the other hand, in the presence of H_2, the reaction rate remarkably increased with Ag/Al ratio. It should be noted that reaction order for NO reduction with respect to the Ag/Al ratio is above 1.

3.5. Influence of concentrations of C_3H_8 and NO

Figs. 10A and 10B show UV-vis spectra of Ag-MFI-58 after treatment in a flow of NO + C_3H_8 + O_2 with various C_3H_8 concentrations at 573 K in the absence and presence of 0.5% of H_2, respectively. In the absence of H_2 (Fig. 10A), Ag^+ ion (210 nm) was the predominant Ag species regardless of C_3H_8 concentration. Even in the presence of H_2 (Fig. 10B), Ag was not agglomerated in the case of a C_3H_8 concentration of 0% (NO + O_2 + H_2). Bands due to $Ag_n^{\delta+}$ clusters appeared by the addition of C_3H_8 in the presence

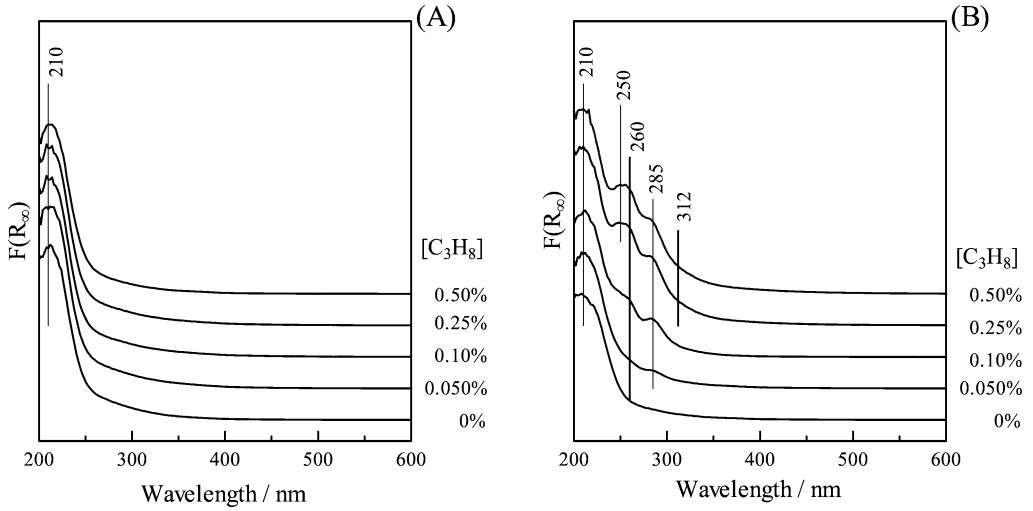

Fig. 10. UV-vis spectra of Ag-MFI-58 after a flow of NO + O_2 + C_3H_8 in the (A) absence and (B) presence of H_2 at 573 K for 30 min. C_3H_8 concentration was varied from 0 to 0.5%. Conditions: NO = 0.1%, O_2 = 10%, and H_2 = 0.5%.

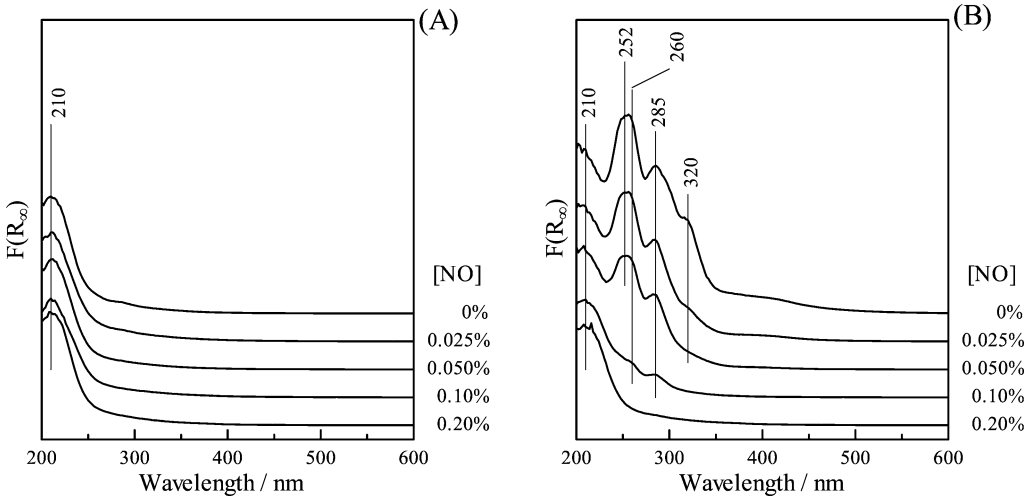

Fig. 11. UV-vis spectra of Ag-MFI-58 after a flow of NO + O_2 + C_3H_8 in the (A) absence and (B) presence of H_2 at 573 K for 30 min. NO concentration was varied from 0 to 0.2%. Conditions: C_3H_8 = 0.1%, O_2 = 10%, and H_2 = 0.5%.

of H_2, and their band intensities increased with an increase in C_3H_8 concentration until 0.1%. Above a C_3H_8 concentration of 0.25%, the band due to metallic a Ag_m cluster (250 and 312 nm) appeared.

Figs. 11A and 11B show UV-vis spectra of Ag-MFI-58 after treatments in a flow of NO + C_3H_8 + O_2 with various NO concentrations at 573 K in the absence and presence of 0.5% of H_2, respectively. In the absence of H_2 (Fig. 11A), Ag^+ ion (210 nm) was the predominant Ag species independent of NO concentration. This includes the case of a NO concentration of 0% (C_3H_8 + O_2). In the presence of H_2 (Fig. 11B), bands due to the $Ag_n^{\delta+}$ cluster (260 and 285 nm) and the metallic Ag_m cluster (252 and 320 nm) were observed in the case of a NO concentration of 0% (C_3H_8 + O_2 + H_2). These bands decreased with an increase in NO concentration. Under the condition of 0.1% of NO, the bands of the metallic Ag_m cluster disappeared, and those of the $Ag_n^{\delta+}$ cluster remained. Disappearance of the bands due to the $Ag_n^{\delta+}$ cluster occurred under the condition of 0.2% of NO. In this case, Ag^+ ion was predominant Ag species.

4. Discussion

4.1. Active species for SCR by C_3H_8 in the presence of H_2 over Ag-MFI at lower temperatures

As shown in Fig. 1A, the lower temperature SCR activity of Ag-MFI below 673 K was enhanced by the addition of H_2. Since there was no NO conversion in a flow of NO + O_2 + H_2, H_2 does not act as a reducing agent of NO but promoter of the SCR by C_3H_8. Promotion of C_3H_8 oxidation by H_2 was confirmed by NO + C_3H_8 + O_2 reaction (Fig. 1B) and C_3H_8 + O_2 reaction (Fig. 2). C_3H_8 conversions in the absence of NO were lower than those in the presence of NO regardless of the presence of H_2 (Fig. 2). This indi-

cates that C_3H_8 is oxidized not only by O_2 but also by NO_x species. These results are similar to those over Ag/Al_2O_3 in our previous reports [13,14]. We reported that the enhancement of NO reduction activity by H_2 over Ag/Al_2O_3 was attributed to the promotion of partial oxidation of C_3H_8 by surface nitrates to mainly surface acetate that is related to rate-determining step of HC-SCR [14]. The promotion of C_3H_8 oxidation by H_2 (Figs. 1b and 2) suggests that the presence of H_2 enhances the lower temperature activity of NO reduction of Ag-MFI through the promotion of partial oxidation of C_3H_8 similar to Ag/Al_2O_3.

The C_3H_8-SCR activity of H-MFI was not enhanced by the addition of H_2, though that of Ag-MFI increased (Fig. 9). This result clearly indicates that modification of Ag species by H_2 leads to the enhancement of NO reduction activity through promotion of the partial oxidation of C_3H_8. Various Ag species such as Ag^+ ion, $Ag_n^{\delta+}$ clusters, metallic Ag_m clusters, and Ag metal are formed under the SCR atmosphere. The C_3H_8-SCR activity of Ag-MFI at lower temperatures strongly depends on Ag species. Ag^+ ion was dominant under the C_3H_8-SCR atmosphere in the absence of H_2 (spectrum b in Fig. 4). The C_3H_8-SCR activity of Ag-MFI was very low in the absence of H_2 (Figs. 1 and 3). These results indicate that Ag^+ ion are not effective for the SCR by C_3H_8. In addition, the NO reaction rate decreased linearly with the increase in Ag/Al ratio in the absence of H_2. Considering that the acid amount is the controlling factor for this reaction over H-form zeolites [37], our present result suggests that the acid site, possibly Brønsted acidic bridging hydroxyl groups, is more active for the SCR by C_3H_8 than Ag^+ ion at low temperatures (Fig. 9).

Our result is in contrast to the previously reported results on Ag catalysts [8,20,27,38]. The SCR activity of Ag/Al_2O_3 by higher hydrocarbons and ethanol is very high at lower temperatures below 700 K. We reported that Ag^+ ion was responsible for selective reduction of NO to N_2 by higher alkanes such as *n*-octane over Ag/Al_2O_3 [27]. High activity of the oxidized state of Ag was reported in the studies for SCR by ethanol [38] over Ag/Al_2O_3. For the SCR by light hydrocarbons, the good ability of Ag^+ ion is exhibited at higher temperatures [8,20]. Li and Flytzani-Sterhanopoulos reported the good ability of Ag^+ ion for the CH_4-SCR over Ag-MFI and Ag-Ce-MFI above 723 K [8]. A similar result was obtained for the C_3H_6-SCR above 673 K over Ag/Al_2O_3 [20]. The difference between our results and those above could be explained as follows. With highly reactive reductants such as *n*-octane and ethanol, the SCR proceeds effectively in the oxidized state such as Ag^+ ion because of the ease of hydrocarbon oxidation. However, light hydrocarbons such as C_3H_8 are more difficult to be oxidized than higher alkanes and ethanol, and temperatures above 700 K are required for activation of C_3H_8. Therefore, Ag^+ ion do not act as an active species for the SCR by light hydrocarbons such as C_3H_8 at lower temperatures.

As shown in Figs. 4 and 6, it is found that Ag^+ ion are reduced and agglomerated to $Ag_n^{\delta+}$ clusters by the addition of H_2 until 1% under the SCR reaction atmosphere. It is very surprising that Ag^+ ion are reduced and agglomerated by 0.5% H_2, although the SCR reaction mixture is overwhelmingly oxidative atmosphere (10% O_2). Assuming that the $Ag_n^{\delta+}$ cluster is composed of four Ag atoms, cluster size is estimated as 5.4 Å from the report by Xu and Kevan [39]. This size is close to the pore diameter of MFI (5.3×5.6 Å in the main channel [40]), which suggests that the $Ag_n^{\delta+}$ cluster is located in the channel of MFI. The SCR activity was increased by the addition of H_2 (Fig. 3). Moreover, the band intensities of the $Ag_n^{\delta+}$ cluster (Fig. 6) and the conversions of NO and C_3H_8 (Fig. 5) increased with the increase in H_2 concentration until 1% where metallic a Ag_m cluster and Ag metal were not formed. The increase in the conversions of NO and C_3H_8 corresponded to an increase in the band intensities of the $Ag_n^{\delta+}$ cluster. These results indicate that the $Ag_n^{\delta+}$ cluster, agglomerated through reduction with H_2 in the channel of MFI, is a highly active species for the C_3H_8-SCR at lower temperatures. The high NO reduction activity of the $Ag_n^{\delta+}$ cluster is supported in the report by Sato et al. for the decane-SCR over Rh-promoted Ag/Al_2O_3 [29].

Further reduction and agglomeration of Ag species result in a drop of the SCR activity and selectivity. Metallic Ag_m clusters and Ag metal particles were observed under the C_3H_8-SCR in the presence of H_2 above 1% (Fig. 6). A metallic Ag_m cluster can be located in the channel of MFI because its size is close to that of a $Ag_n^{\delta+}$ cluster, while Ag metal particles are clearly located on external surface of MFI. The NO reduction activity and selectivity declined under the SCR condition of H_2 concentration above 1% where a metallic Ag_m cluster was formed (Fig. 5). Moreover, after treatment in 100% H_2 at 773 K, a metallic Ag_m cluster and Ag metal were also observed (Fig. 8), and the initial SCR activity was nearly zero while the initial conversion of C_3H_8 was 34% (Fig. 7). These results indicate that the much agglomerated Ag species, that is, metallic Ag_m clusters and Ag metal are not active for the C_3H_8-SCR but for nonselective hydrocarbon combustion. The ability of metallic Ag_m clusters and Ag metal in hydrocarbon combustion is supported in the literature [19,20,38,41].

In addition, NO conversion and selectivity after pretreatment in 100% H_2 increased with time on stream as shown in Fig. 7. UV-vis spectroscopy revealed that the bands of the $Ag_n^{\delta+}$ cluster appeared at the expense of the disappearance of those of the metallic Ag_m cluster and Ag metal with time on stream. These results indicate that transformation of metallic Ag_m clusters and Ag metal to $Ag_n^{\delta+}$ clusters, which are highly active species for the C_3H_8-SCR, leads to the enhancement of NO reduction activity and selectivity.

From the above discussion, it is concluded that the addition of H_2 leads to the enhancement of the lower temperature C_3H_8-SCR activity of Ag-MFI through the formation of $Ag_n^{\delta+}$ clusters by moderate agglomeration of Ag^+ ions. This high NO reduction activity of a $Ag_n^{\delta+}$ cluster is attributed to the higher ability of C_3H_8 partial oxidation than Ag^+ ions and higher selectivity than to Ag_m clusters and

Ag metal. This conclusion in Ag-MFI should be applied to Ag/Al_2O_3 in which the addition of H_2 leads to the promotion of the C_3H_8-SCR.

4.2. Influence of Ag content on SCR by C_3H_8 in the presence of H_2

As shown in Fig. 9, the reaction rate of NO remarkably increased with the Ag/Al ratio in the presence of H_2 with a reaction order above 1. If the active species of the C_3H_8-SCR is composed of a single atom of Ag such as Ag^+ ion, the reaction order for NO reduction should be equal to 1. Therefore, the dependence above first order of the NO reaction rate on Ag/Al ratio also supports that Ag^+ ion are not active species for the C_3H_8-SCR at lower temperatures. Beyer and Jacobs proposed following mechanism (Eqs. (1)–(3)) for the reduction of Ag^+ ion to $(Ag_2{}^+)_m$ by H_2 from kinetic analysis of the uptake of H_2 over Ag-chabasites [36]:

$$H_2 \leftrightarrows 2H, \tag{1}$$

$$H + Ag^+ \leftrightarrows [Ag^0H^+], \tag{2}$$

$$[Ag^0H^+] + Ag^+ \rightarrow Ag_2^+ + H^+. \tag{3}$$

In Eqs. (2) and (3), Ag^+, $Ag_2{}^+$, and H^+ can be located on ion-exchanged sites. They concluded that the rate-determining step is Eq. (3), and the kinetic equation is expressed as

$$R = k[Ag^+]^2[H_2]^{0.5}. \tag{4}$$

According to Eq. (4), the reduction rate of Ag^+ ion is proportional to the Ag^+ concentration squared. The formation of $Ag_n{}^{\delta+}$ clusters in our catalytic system should also proceed through a mechanism similar to the above one. Therefore, the concentration of a $Ag_n{}^{\delta+}$ cluster can be influenced by the rate described in Eq. (4), and can be proportional to the above first power of Ag/Al ratio. From the above discussion, the dependence above first order of the NO reaction rate on the Ag/Al ratio rationalizes that $Ag_n{}^{\delta+}$ clusters are the active species for C_3H_8-SCR over Ag catalysts in the presence of H_2.

4.3. Balance of various Ag species under SCR atmosphere

As shown in Fig. 4, the formation of a $Ag_n{}^{\delta+}$ cluster by the addition of H_2 was reversible. Considering the higher activity of $Ag_n{}^{\delta+}$ clusters than Ag^+ ion, the response of NO conversions by the addition and removal of H_2 (Fig. 3) strongly suggests that both agglomeration of Ag^+ ion to $Ag_n{}^{\delta+}$ clusters and dispersion of $Ag_n{}^{\delta+}$ clusters to Ag^+ ion should be very fast. Actually, fast agglomeration of Ag^+ ions to Ag clusters, with an absorption band at 306 nm, and fast dispersion of Ag clusters to Ag^+ ion was confirmed by an in situ UV-vis study on Ag/Al_2O_3 [18]. This fast transformation means that the balance of Ag^+ ion and $Ag_n{}^{\delta+}$ clusters shifts immediately in varying SCR atmosphere.

Metallic Ag_m clusters and Ag metals were transformed to $Ag_n{}^{\delta+}$ clusters under a flow of NO + C_3H_8 + O_2 + H_2 (Fig. 8). This result indicates that metallic Ag_m clusters and Ag metal are oxidized under an SCR atmosphere. The slower oxidation of Ag metal than $Ag_n{}^{\delta+}$ clusters implies a difficulty in migration from the external surface into an internal one of MFI. On the other hand, metallic Ag_m clusters and Ag metal were formed by H_2 at lower temperatures as reported in previous literature [15–17]. For example, Baker et al. reported that $Ag_m{}^0$ microclusters (size below 5 nm) on the external surface of Y zeolites were formed by the treatment of dehydrated Ag-Y with H_2 at 423–473 K [16]. The behavior of metallic Ag_m clusters and Ag metal as described above indicates that the formation of metallic Ag_m clusters and Ag metal is reversible, which suggests that the balance of $Ag_n{}^{\delta+}$ clusters, metallic Ag_m clusters, and Ag metal shifts in varying SCR atmosphere. No detection of a Ag metal band in UV-vis spectra in Figs. 4, 6, 10, and 11 should be attributed to a much slower formation rate of Ag metal by reductants than to the disappearance rate of Ag metal by oxidants.

The composition of reaction gas mixture shifts the balance of Ag species on Ag-MFI. As discussed above, H_2 acts as a reductant of Ag species. Moreover, C_3H_8 and NO act as a reductant and an oxidant of Ag species, respectively, as shown by UV-vis spectra after the SCR at various C_3H_8 (Fig. 10B) and NO concentrations (Fig. 11B) in the presence of H_2. Ag^+ ion was predominant Ag species on Ag-MFI in a flow of C_3H_8 + O_2 (Fig. 11A). This result indicates that the ability of O_2, as an oxidant is higher than that of C_3H_8 as a reductant. The roles of NO, O_2 and H_2 were confirmed in our in situ UV study of Ag/Al_2O_3 [18]. In the absence of H_2, Ag^+ ion was predominant Ag species independent of C_3H_8 (Fig. 10A) and NO concentrations (Fig. 11A). This should be attributed to a much higher ability of NO and O_2 to oxidize Ag species than that of C_3H_8 to reduce Ag species.

From the above discussion, Ag species in MFI zeolite are balanced as described in Eq. (5) during the SCR by C_3H_8. In the absence of H_2, the balance shifts to the left because of the poor ability of C_3H_8 as a reductant of Ag species. The addition of H_2 shifts the balance to the right. A moderate balance between gaseous oxidants and reductants is important for the formation of $Ag_n{}^{\delta+}$ clusters, which are active species for the SCR by C_3H_8,

$$\begin{aligned} Ag^+ \text{ ion} &\overset{H_2,C_3H_8}{\underset{NO,O_2}{\leftrightarrows}} Ag_n{}^{\delta+} \text{ cluster} \\ &\overset{H_2,C_3H_8}{\underset{NO,O_2}{\leftrightarrows}} Ag_m \text{ cluster, Ag metal.} \end{aligned} \tag{5}$$

5. Conclusions

The lower temperature C_3H_8-SCR activity of Ag ion-exchanged MFI-type zeolites was enhanced significantly by the addition of H_2. Ag species after the SCR by C_3H_8 in the absence and presence of H_2 was investigated with UV-vis

spectroscopy, and the promotion effect of H_2 on the SCR by C_3H_8 was discussed from the viewpoint of active Ag species. The various Ag species (Ag^+ ion, $Ag_n^{\delta+}$ clusters ($2 \leqslant n \leqslant 4$), metallic Ag_m clusters ($3 \leqslant m \leqslant 5$), and Ag metal) are in existence during the SCR by C_3H_8 depending on the gaseous composition, and the balance among Ag species is changed by the gaseous composition. This balance lies to Ag^+ ion in the absence of H_2. The addition of H_2 shifts remarkably the balance to $Ag_n^{\delta+}$ clusters and metallic Ag_m clusters. It is concluded that $Ag_n^{\delta+}$ clusters, formed reversibly through the reductively moderate agglomeration by H_2, lead to the enhancement of the C_3H_8-SCR through the promotion of C_3H_8 partial oxidation.

Acknowledgments

This work was partly supported by a Grant-in-Aid from the Ministry of Education, Science and Culture, Japan. The authors thank Dr. K. Itabashi of Tosoh Co. for providing zeolite samples.

References

[1] M. Iwamoto, H. Yahiro, Y. Yu-u, S. Shundo, N. Mizuno, Shokubai (Catalyst) 32 (1990) 430.
[2] W. Held, A. König, T. Richter, L. Pupper, SAE Paper 900496 (1990).
[3] M. Shelef, Chem. Rev. 95 (1995) 209.
[4] M. Iwamoto, H. Yahiro, Catal. Today 22 (1994) 5.
[5] Y. Traa, B. Burger, J. Weitkamp, Micropor. Mesopor. Mater. 30 (1999) 3.
[6] T. Miyadera, Appl. Catal. B 2 (1993) 199.
[7] Z. Li, M. Flytzani-Sterhanopoulos, Appl. Catal. A 165 (1997) 15.
[8] Z. Li, M. Flytzani-Sterhanopoulos, J. Catal. 182 (1999) 313.
[9] K. Masuda, K. Tsujimura, K. Shinoda, T. Kato, Appl. Catal. B 8 (1996) 33.
[10] K. Masuda, K. Shinoda, T. Kato, K. Tsujimura, Appl. Catal. B 15 (1998) 29.
[11] A. Shichi, Y. Kawamura, A. Satsuma, T. Hattori, Stud. Surf. Sci. Catal. 135 (2001) 172.
[12] S. Satokawa, Chem. Lett. (2000) 294.
[13] S. Satokawa, J. Shibata, K. Shimizu, A. Satsuma, T. Hattori, Appl. Catal. B 42 (2003) 179.
[14] J. Shibata, K. Shimizu, S. Satokawa, A. Satsuma, T. Hattori, Phys. Chem. Chem. Phys. 5 (2003) 2154.
[15] H. Beyer, P.A. Jacobs, J.B. Uytterhoeven, J. Chem. Soc., Faraday Trans. 1 72 (1976) 674.
[16] M.D. Baker, G.A. Ozin, J. Godber, J. Phys. Chem. 89 (1985) 305.
[17] T. Baba, N. Akinaka, M. Nomura, Y. Ono, J. Chem. Soc., Faraday Trans. 89 (1993) 595.
[18] A. Satsuma, J. Shibata, A. Wada, Y. Shinozaki, T. Hattori, Stud. Surf. Sci. Catal. 145 (2003) 235.
[19] N. Bogdanchikova, F.C. Meunier, M. Avalos-Borja, J.P. Breen, A. Pestryakov, Appl. Catal. B 36 (2002) 287.
[20] K.A. Bethke, H.H. Kung, J. Catal. 172 (1997) 93.
[21] N.E. Bogdanchikova, M.N. Dulin, A.V. Toktarev, G.B. Shevnina, V.N. Kolomiichuk, V.I. Zaikovskii, V.P. Petranovskii, Stud. Surf. Sci. Catal. 84 (1994) 1067.
[22] M. Matsuoka, E. Matsuda, K. Tsuji, H. Yamashita, M. Anpo, J. Mol. Catal. A 107 (1996) 399.
[23] J. Texter, T. Gonsiorowski, R. Kellerman, Phys. Rev. B 23 (1981) 4407.
[24] J. Michalik, J. Sadlo, T. Kodaira, S. Shimomura, H. Yamada, J. Radioanal. Nucl. Chem. 232 (1998) 135.
[25] G.A. Ozin, M.D. Baker, J. Godber, J. Phys. Chem. 88 (1984) 4902.
[26] K. Shimizu, H. Maeshima, A. Satsuma, T. Hattori, Appl. Catal. B 18 (1998) 163.
[27] K. Shimizu, J. Shibata, H. Yoshida, A. Satsuma, T. Hattori, Appl. Catal. B 30 (2001) 151.
[28] Z.M. Wang, M. Yamaguchi, I. Goto, M. Kumagai, Phys. Chem. Chem. Phys. 2 (2000) 3007.
[29] K. Sato, T. Yoshinari, Y. Kintaichi, M. Haneda, H. Hamada, Appl. Catal. B 44 (2003) 67.
[30] J. Texter, J.J. Hastreiter, J.L. Hall, J. Phys. Chem. 87 (1983) 4690.
[31] P. Mulvaney, A. Henglein, J. Phys. Chem. 94 (1990) 4182.
[32] T. Linnert, P. Mulvaney, A. Henglein, H. Weller, J. Am. Chem. Soc. 112 (1990) 4657.
[33] B.G. Ershov, E. Janata, A. Henglein, J. Phys. Chem. 97 (1993) 339.
[34] E. Gachard, J. Belloni, M.A. Subramanian, J. Phys. Chem. 6 (1996) 867.
[35] S.A. Mitchell, G.A. Ozin, J. Phys. Chem. 88 (1984) 1425.
[36] H.K. Beyer, P.A. Jacobs, Stud. Surf. Sci. Catal. 12 (1982) 95.
[37] A. Satsuma, M. Iwase, A. Shichi, T. Hattori, Y. Murakami, Stud. Surf. Sci. Catal. 105 (1997) 1533.
[38] N. Aoyama, K. Yoshida, A. Abe, T. Miyadera, Catal. Lett. 43 (1997) 249.
[39] B. Xu, L. Kevan, J. Phys. Chem. 95 (1991) 1147.
[40] Ch. Baerlocher, W.M. Meier, D.H. Olson, Atlas of Zeolite Framework Types, fifth revised Ed., Elsevier, Amsterdam, 2001, p. 184.
[41] F.C. Meunier, J.P. Breen, V. Zuzaniuk, M. Olsson, J.R.H. Ross, J. Catal. 187 (1999) 493.